

# Out-of-plane seismic failure assessment of spandrel walls in long-span masonry stone arch bridges using cohesive interface

Alemdar Bayraktar<sup>\*1</sup>, Emin Hökelekli<sup>2a</sup>, Meral Halifeoğlu<sup>3b</sup>, Zülfikar Halifeoğlu<sup>4c</sup> and Ashraf Ashour<sup>5d</sup>

<sup>1</sup>Department of Civil Engineering, Karadeniz Technical University, Turkey

<sup>2</sup>Department of Civil Engineering, Bartın University, Bartın, Turkey

<sup>3</sup>Department of Civil Engineering, Dicle University, Diyarbakır, Turkey

<sup>4</sup>Senior Civil Engineering, Zülfikar Halifeoglu Company, Diyarbakır, Turkey

<sup>5</sup>University of Bradford, Bradford, West Yorkshire, U.K.

(Received October 16, 2019, Revised September 12, 2019, Accepted September 12, 2019)

**Abstract.** The main structural elements of historical masonry arch bridges are arches, spandrel walls, piers and foundations. The most vulnerable structural elements of masonry arch bridges under transverse seismic loads, particularly in the case of out-of-plane actions, are spandrel wall. The vulnerability of spandrel walls under transverse loads increases with the increasing of their length and height. This paper computationally investigates the out-of-plane nonlinear seismic response of spandrel walls of long-span and high masonry stone arch bridges. The Malabadi Bridge with a main arch span of 40.86m and rise of 23.45m built in 1147 in Diyarbakır, Turkey, is selected as an example. The Concrete Damage Plasticity (CDP) material model adjusted to masonry structures, and cohesive interface interaction between the infill and the spandrel walls and the arch are considered in the 3D finite element model of the selected bridge. Firstly, mode shapes with and without cohesive interfaces are evaluated, and then out-of-plane seismic failure responses of the spandrel walls with and without the cohesive interfaces are determined and compared with respect to the displacements, strains and stresses.

**Keywords:** long-span masonry arch bridge; out-of-plane response; seismic failure; masonry spandrel wall; transverse behavior

## 1. Introduction

Masonry arch bridges have different structural elements shown in Fig. 1. The voussoirs or the bricks are supported upon the skewback at a surface named springing. The spandrel walls restrain the fill and carry the parapets and also stiffen and strengthen the arch barrel as a whole. The wing walls are built by extending the spandrels on each side of the arch to resist the outward pressures from the backfill. The backfill is usually made up of soil or mortared rubble as shown in Fig. 2.

There are thousands of road and railway masonry arch bridges in the world, and large numbers of old masonry bridges are still in use. The effects such as traffic loads and vibrations, environmental conditions (wind, rain, frost attack, high/low temperature cycles, moisture), extreme natural events (earthquakes, river overflows, floods)

progressively induce material deterioration, damage development (opening of joints and ring separation in arch barrels, cracks in piers, wing walls and parapets, loss of bricks and mortar joints) and deformations (distortion of the arch profile, out-of-plane rotation of spandrel walls) (Sarhosis *et al.* (2016)). Some of these effects were investigated by many researchers in the literature. A comprehensive review of experimental investigations and assessment methods of masonry arch bridges until year of 2016 is summarized by Sarhosis *et al.* (2016). Bayraktar and his colleagues have investigated the response of various masonry arch bridges in Turkey (Bayraktar *et al.* 2009, 2010, 2015, Altunışık *et al.* 2011, 2015, Sevim *et al.* 2011a, 2011b, 2016). Furthermore, Lancioni *et al.* (2016) determined seismic vulnerability of ancient stone arches by using a numerical model based on the Non-Smooth Contact Dynamics method. Gullu and Jaf (2016) performed full 3D nonlinear time history analysis of a historical masonry arch bridge considering dynamic soil–structure interaction. Stavroulaki *et al.* (2016) implemented modeling and strength evaluation of masonry bridges using terrestrial photogrammetry and finite element analysis. It was emphasized that the variation of the elasticity modulus of the fill may significantly influence the values of crack opening of the masonry arch bridge. Costa *et al.* (2016) performed calibration of the numerical model of a stone masonry railway bridge based on experimentally identified modal parameters. Cavalagli *et al.* (2016) determined lateral loads carrying capacity and minimum thickness of circular

\*Corresponding Author, Emeritus Professor

Email: [alemdarbayraktar@gmail.com](mailto:alemdarbayraktar@gmail.com)

<sup>a</sup>Assistant Professor

Email: [emin\\_hokelekli@hotmail.com](mailto:emin_hokelekli@hotmail.com)

<sup>b</sup>Associate Professor

Email: [mhalife@gmail.com](mailto:mhalife@gmail.com)

<sup>c</sup>Senior Civil Engineer

Email: [z.halifeoglu@hotmail.com](mailto:z.halifeoglu@hotmail.com)

<sup>d</sup>Professor

Email: [A.F.Ashour@bradford.ac.uk](mailto:A.F.Ashour@bradford.ac.uk)

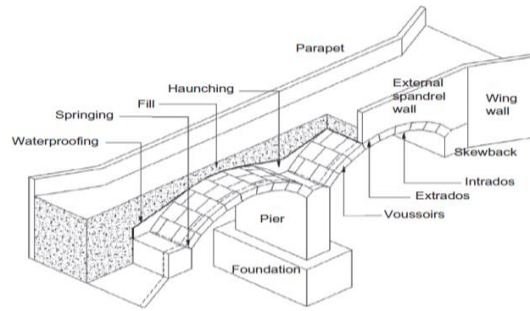


Fig. 1 Main structural elements of a masonry arch bridge (UIC Code 778–3R, 1994)



Fig. 2 Views from spandrel walls with soil and mortared rubble backfills

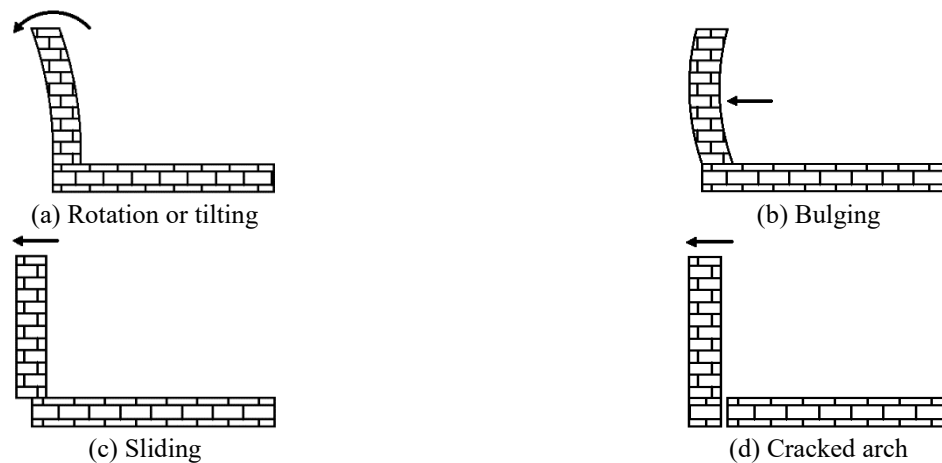


Fig. 3 Out-of-plane failure modes of spandrel walls (Page 1993, Thompson 1995, Chajes 2002)

and pointed masonry arches. Ataei *et al.* (2017) performed assessment of load carrying capacity enhancement of an open spandrel masonry arch bridge by dynamic load testing. Martinelli *et al.* (2017) determined bearing capacity assessment of a 14th century arch bridge in Lecco (Italy). Karaton *et al.* (2017) investigated nonlinear seismic performance of a 12th century historical masonry bridge under different earthquake levels. Moreira *et al.* (2017) implemented probabilistic-based assessment of a masonry arch bridge considering inferential procedures. Zampieri *et al.* (2018) investigated collapse mechanisms of masonry arches with settled springing considering different geometrical configurations and settlement directions. Severini *et al.* (2018) determined dynamic response of circular masonry arch with geometrical irregularities subjected to a pulse-type ground motion. Zhang *et al.* (2018) investigated the effects of various parameters, including masonry bond and defects in the brickwork, abutment stiffness and movements at the supports, which

are usually disregarded in practical assessment of masonry arch bridges. Aydın and Özkaya (2018) performed finite element analysis of collapse loads of single-spanned historic masonry arch bridge named as Sarpdere Bridge.

Naderi and Zekavati (2018) investigated seismic behavior of a masonry stone bridge using finite element and discrete element methods. It was emphasized that combination of these methods is an efficient technique for the analyses of masonry stone bridges. Michiels and Adriaenssens (2018) developed form-finding algorithm for masonry arches subjected to earthquake loading. New material-efficient arch shapes were obtained by considering both horizontal and gravitational acceleration in the form finding process for different horizontal accelerations and for arches of different rise-to-span ratios.

The above mentioned studies generally focused on the static and earthquake responses of masonry arches. However, masonry spandrel walls are particularly vulnerable to the application of loads in the transverse



Fig. 4 Some views from spandrel wall failures after earthquakes (Rota (2004))

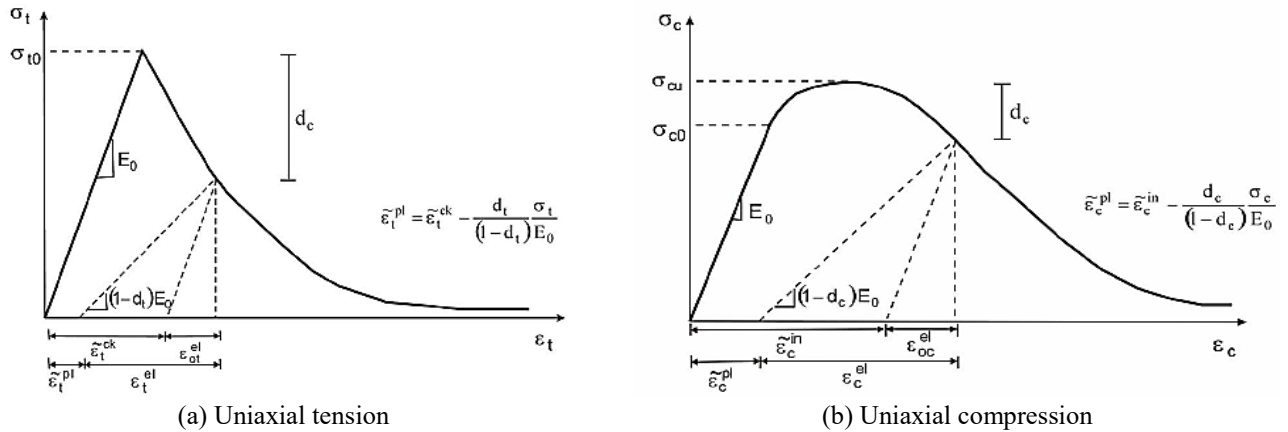


Fig. 5 Concrete damage plasticity (CDP) stress-strain diagrams (Abaqus (2010))

direction (Casolo 1999, Erdogmus and Boothby 2004, Shi 2016). There are four failure modes for spandrel walls such as bulging, rotation or tilting, sliding and cracked arch as shown in Fig. 3.

These failures are a local mechanism, and generally do not involve the structural safety of the arch, but it can compromise the support of the ballast and the rail tracks, and in the end the serviceability of the bridge (Porto *et al.* 2016). The importance of transverse effects in the seismic responses of spandrel walls in long and high masonry arch bridges were emphasized by Fanning *et al.* (2001), Rota *et al.* (2005), Zampieri *et al.* (2015) and Sarhosis *et al.* (2016). Some views from the failures of spandrel walls in masonry arch bridges subjected to transverse earthquake forces are shown in Fig. 4.

The out-of-plane seismic responses of spandrel walls with cohesive interface in long-span and high masonry arch bridges have not been widely addressed in the literature. This paper aims to investigate numerically the out-of-plane seismic failure responses of spandrel walls with cohesive interface in long-span and high masonry stone arch bridges. For this purpose, Malabadi Bridge with a main arch span of 40.86 m and a height of 23.45 m built in 1147 in Diyarbakır, Turkey, is selected as an example. The Concrete Damage Plasticity (CDP) material model adjusted to masonry structures and cohesive interface interaction between the infill and the spandrel walls and the arch are considered in the 3D finite element model of the bridge. The modal and out-of-plane seismic failure responses of the spandrel walls with and without cohesive interface interactions are determined and compared with each other.

## 2. Masonry unit and interface interaction models

### 2.1 Material model for masonry units

A masonry arch bridge is a three-dimensional (3D) heterogeneous structure, where different structural components perform their own function within the integral system and cooperate with each other to guarantee an adequate structural performance. Therefore, for a realistic prediction of the bridge response up to collapse, a numerical simulation capable of representing the nonlinear behavior of the main bridge components (e.g., masonry arch, spandrel walls and backfill) as well as their mutual interaction is required. However, the accuracy of the response prediction for masonry arch bridges is mainly associated with the ability of the adopted mechanical model to represent material nonlinearity in masonry.

Drucker-Prager, Extended Drucker-Prager, Mohr-Coulomb and Concrete Damage Plasticity material models (Öztürk *et al.* 2019) are generally used in nonlinear material analyses of masonry arch bridges. Arches and spandrel walls of the selected Malabadi Bridge in this study were made up of cut stone with mortar, whereas the rubble stones with mortar were used in backfill. Concrete Damage Plasticity (CDP) model for arches, spandrel walls and backfill are chosen as a nonlinear material model in this study. Concrete damage plasticity stress-strain diagrams under uniaxial tension and compression are given in Fig. 5. Material properties of masonry are adapted to the CDP model according to the study carried out by Kaushik *et al.* (2007).

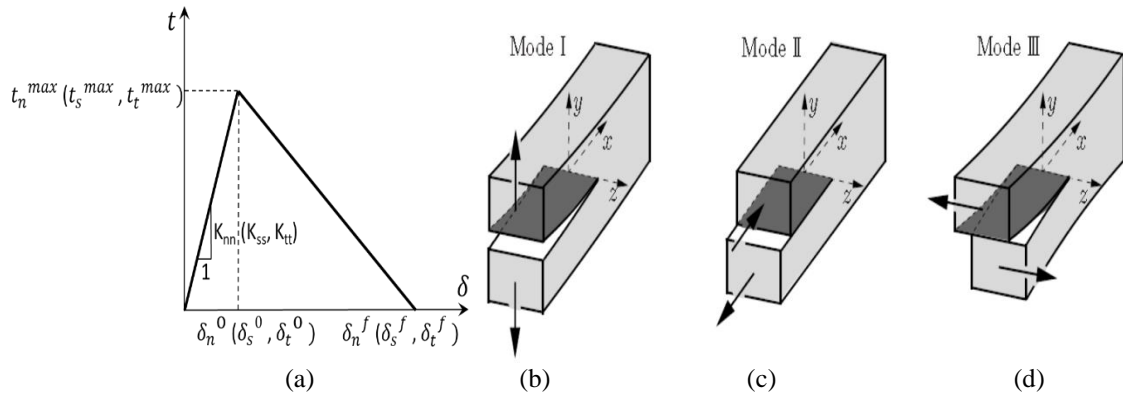


Fig. 6 Traction-separation behaviour (a), opening (b), in-plane shear (c) and out-of-plane shear (d) failure modes of surface-based cohesive contact model (Bolhassani *et al.* (2015), Abdulla *et al.* (2017), Salih (2018))

## 2.2 Cohesive interface model

Masonry arch bridges are heterogeneous systems where the backfill material plays a critical role spreading the loads applied on the road/rail surface below to the arch barrel, while providing transverse resistance and passive pressure to the deformed arch. Thus, a realistic representation of the backfill behavior and its interaction with the arch barrel and spandrel walls is critical for an accurate response prediction of masonry arch bridges. The interactions between stone-to-stone, the backfill-to-spandrel wall and backfill-to-arch were modelled in literature by using interface and cohesive elements (Lourenço and Rots 1997, Fanning *et al.* 2001, Sacco and Toti 2010, Gago *et al.* 2011, and Macorini and Izzuddin 2011).

The surface-based cohesive contact model with rate-dependent behaviors adopted to capture the interaction between the backfill-to-spandrel walls and backfill-to-arch in this study. Traction-separation behavior, normal (opening), in-plane and out-of-plane shear failure modes of the surface-based cohesive contact model are shown in Fig. 6. A detailed description of interface formulations can be found in references (Lourenco 1996, Camanho and Dávila 2002, Abaqus 2010, Kowalewski and Gajewski 2015, Bolhassani *et al.* 2015, Abdulla *et al.* 2017). A brief formulation of the surface-based cohesive contact model will be mentioned here.

The initial relation between the elastic stiffness matrix,  $K$ , traction and separation vectors,  $t$  and  $\delta$ , respectively, of the surface-based cohesive contact model given in Fig. 6 is expressed in Eq. (1).

$$t = \begin{Bmatrix} t_n \\ t_s \\ t_t \end{Bmatrix} = \begin{bmatrix} K_{nn} & 0 & 0 \\ 0 & K_{ss} & 0 \\ 0 & 0 & K_{tt} \end{bmatrix} \begin{Bmatrix} \delta_n \\ \delta_s \\ \delta_t \end{Bmatrix} = K\delta \quad (1)$$

The equivalent stiffness of contact interfaces in the normal ( $K_{nn}$ ) and shear directions ( $K_{ss}$  and  $K_{tt}$ ) are calculated by using Eqs. (2)-(3) (Lourenco 1996).

$$K_{nn} = \frac{E_u E_m}{h_m (E_u - E_m)} \quad (2)$$

$$K_{ss} \text{ and } K_{tt} = \frac{G_u G_m}{h_m (G_u - G_m)} \quad (3)$$

The initial linear response of the interface contact is followed by crack propagation. The quadratic stress criterion expressed as in Eq. (4) is used to define damage initiation; this criterion is met when the quadratic stress ratios of masonry interfaces are equal to one.

$$\left(\frac{t_n}{t_n^{\max}}\right)^2 + \left(\frac{t_s}{t_s^{\max}}\right)^2 + \left(\frac{t_t}{t_t^{\max}}\right)^2 = 1 \quad (4)$$

Once the damage initiation criterion is reached, the propagation of cracks in the contact interfaces causes stiffness degradation at a defined rate which leads to total strength loss and failure of interfaces (Abdulla *et al.* 2017). If Eq. (1) is rewritten for the plastic response

$$t = (1 - D)K\delta \quad (5)$$

where  $D$  is the damage evolution variable, the value increases from 0 to 1 as per continuity of traction stresses after the damage initiation criterion met.

## 3. Application

### 3.1 Malabadi Bridge

Malabadi Bridge constructed in Silvan province of Diyarbakır city, Turkey, was chosen as an application. The historical Malabadi Bridge is located on the Batman Stream pouring into the Dicle River. The bridge was built by Artukoğulları in 1147 (Sert *et al.* 2015, Web-1 2018). Batman Dam, which was built in 2003, is located on the 750 m upstream of the bridge. The bridge is a masonry stone arch bridge with five spans. The length and height of the main span is 40.86 m and 23.45 m, respectively. The main span arch is double-centered and its thickness is 1.54 m. The bridge has a total length of 220 m. The arches and the spandrel walls are constructed using cut stone with mortar. There are chambers in the bridge body in order to reduce the bridge self-weight and, consequently, the foundation load. The last restoration work on the bridge was carried out in 2014. The plan, cross-section and view of Malabadi Bridge are given in Fig. 7.

The bridge foundations are located on the Silvan limestone rocks as shown in Fig. 8. The drill logs were

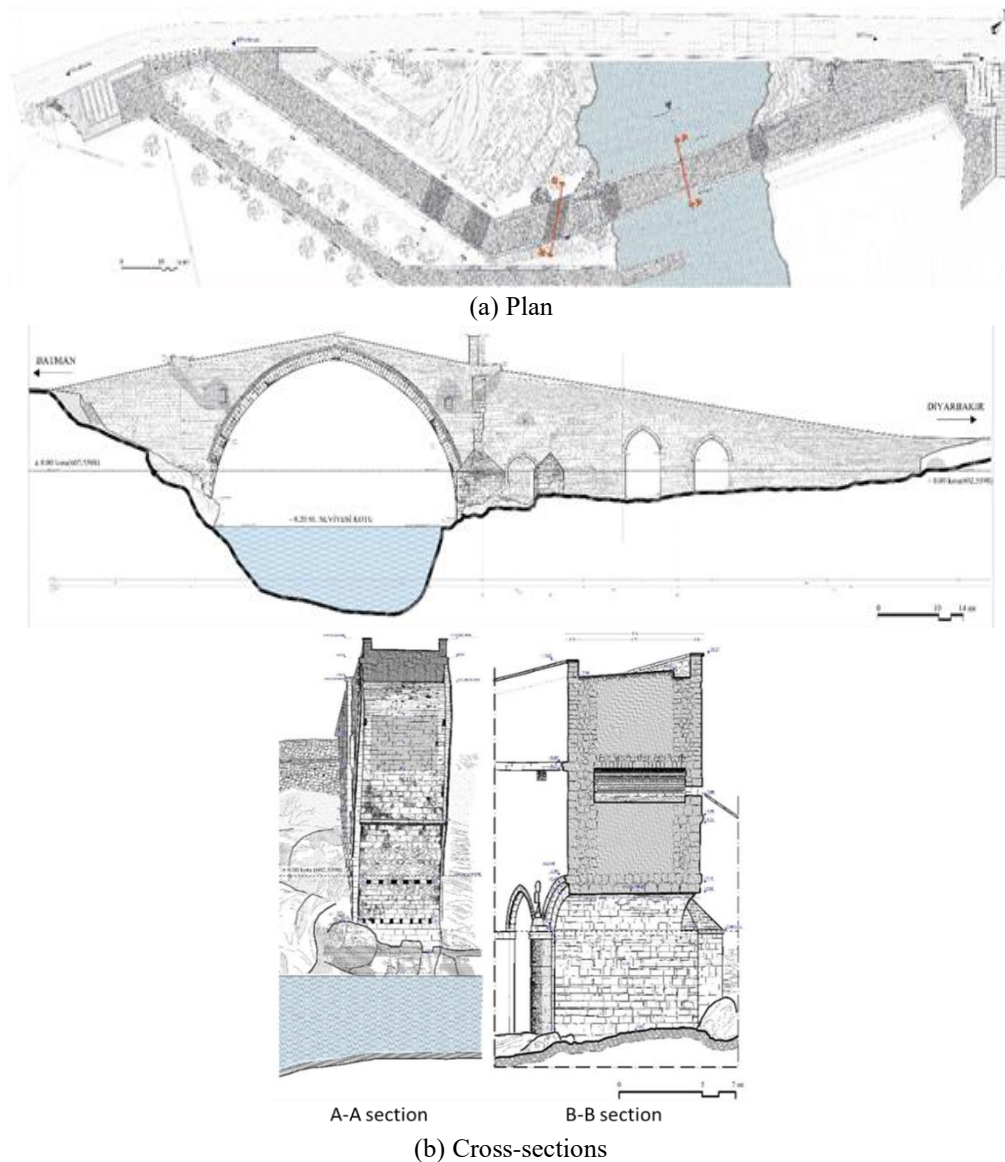


Fig. 7 Plan, cross-sections and view of Malabadi Bridge



Fig. 8 A view from the bridge foundations located on the rock

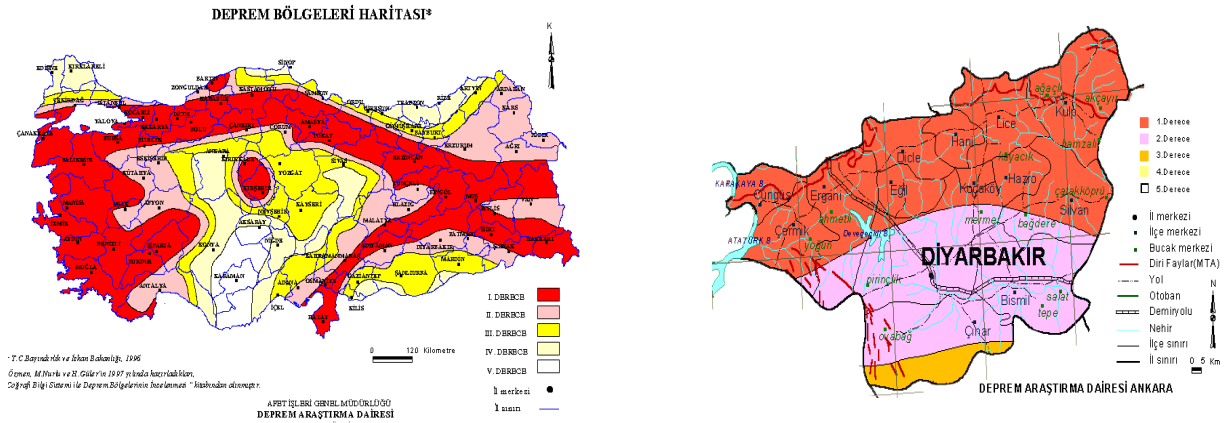
taken and the compressive strength and subgrade modulus of the rock were determined as  $3.72 \text{ N/mm}^2$  and  $14864 \text{ kN/m}^3$ , respectively (Restoration Project 2014).

The site class of the bridge is defined as 'A' and the rock core value (RQD) is 100%. Since the foundation of the bridge is rock, there is no risk of settlement, swelling and liquefaction.

When the bridge area is examined in terms of seismicity, the 1975 Lice ( $M=6.6$ ) and the 2003 Bingöl ( $M=5.9$ ) earthquakes occurred in this region. The active fault and



(a) Active fault map of Turkey (Web-2 (2018))



(b) Earthquake zoning map of Turkey and Diyarbakir (Web-3 (2018))

Fig. 9 Active fault and earthquake zoning maps of Turkey and Diyarbakir

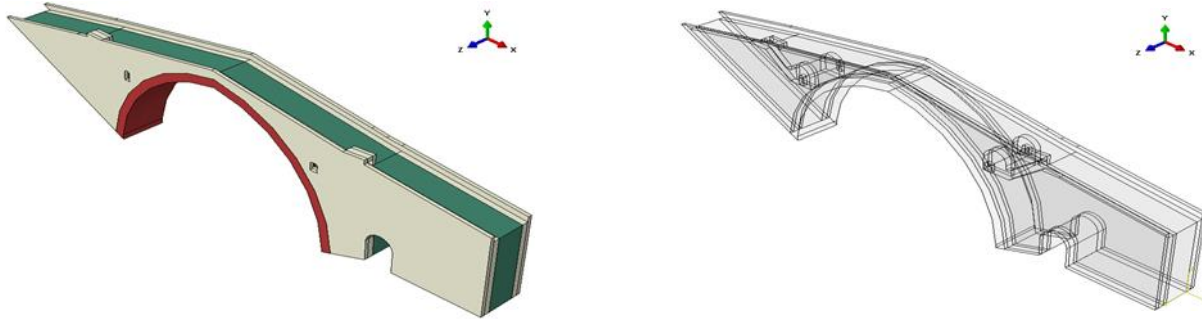


Fig. 10 Solid model of Malabadi Bridge

Table 1 Mechanical properties of masonry and interface unit

Properties	Walls	Backfill	Interface
Modulus of Elasticity (MPa)	7000	1000	
Poisson's ratio	0.20	0.25	
Density (kg/m <sup>3</sup> )	2100	1900	
Compressive Strength (MPa)	7.0	1.0	
Tensile Strength (MPa)	0.3	0.05	
Normal Stiffness (N/mm <sup>3</sup> )			2400
Shear Stiffness (N/mm <sup>3</sup> )			1000

earthquake zoning maps of Turkey and Diyarbakir is shown in Fig. 9. Expected acceleration values for 1st, 2nd, 3rd, 4th and 5th degree earthquake zones in Turkey are more than 0.4 g, between 0.3 g-0.4 g, between 0.2 g-0.3 g, between 0.2 g-0.1 g and less than 0.1 g (where g is the gravity acceleration), respectively. It can also be seen from Fig.

9(b) that Diyarbakir city is in 1st, 2nd and 3rd degree earthquake zones. Malabadi Bridge is in the 1<sup>st</sup> degree earthquake zone.

Limestone was used in the spandrel walls and arches of the bridge. As a result of the tests carried out on the samples taken from the bridge structural elements and mortar, the average compressive strength and the unit weight of the stone were determined as 35 MPa and 21 kN/m<sup>3</sup>, and the mortar strength was obtained as 3.5 MPa (Restoration Project, 82014)). Rubble stones with mortar were used in the backfill as filling material (Fig. 2). The unit weight of filling material was chosen as 19 kN/m<sup>3</sup>. The average mechanical properties of interfaces and the masonry units obtained from the laboratory tests, the relations in Eurocode 6 (1996) and the references (Loo and Yang 1991, Ali and Page 1988, Lourenço and Rots 1997, Doherty 2000, Boothby 2001, Fanning and Boothby 2001, Cavicchi and

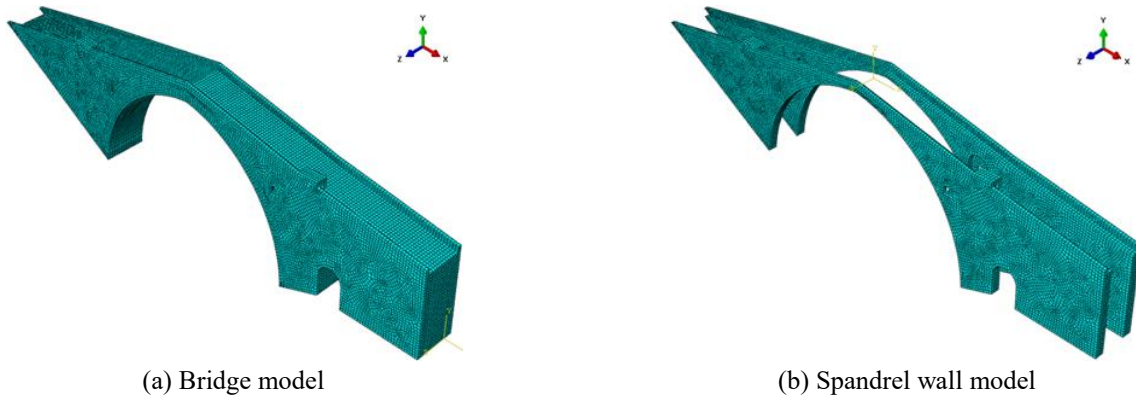


Fig. 11 Finite element model of the bridge

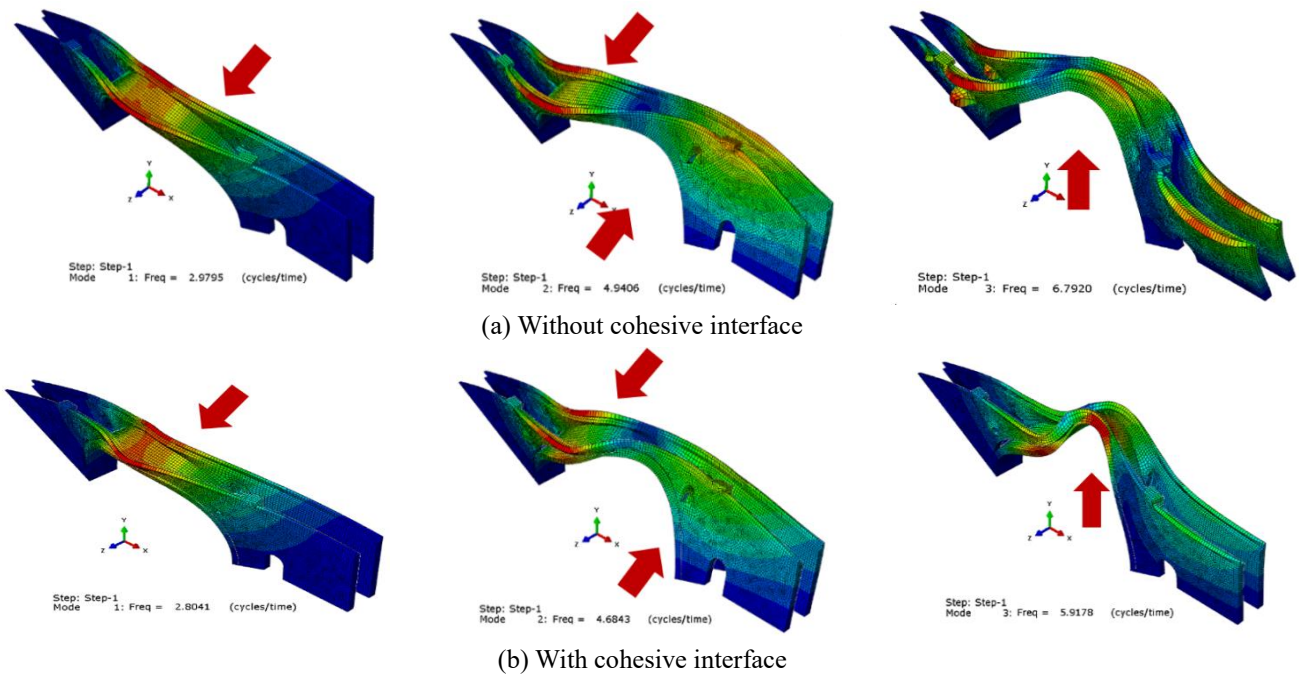


Fig. 12 Mode shapes of the bridge with and without cohesive interfaces between the fill and the spandrel walls and the arches

Gambarotta 2005, 2007, Ordune 2005, Sacco and Toti 2010, Macorini and Izzuddin 2011, Milani and Tralli 2011, Milani and Lourenço 2012, Wang 2014, Bolhassani *et al.* 2015, Zhang 2015, Aras and Altay 2015, Kowalewski and Gajewski 2015, Costa *et al.* 2015) are given in Table 1. The relation ( $f_k = K f_b^\alpha f_m^\beta$ ) in Eurocode 6 (1996) is used for the calculation of compressive strength of the masonry walls, and the values of  $K$ ,  $\alpha$  and  $\beta$  are taken as 0.51, 0.65 and 0.25, respectively. The modulus of elasticity of masonry units is taken as  $1000f_k$ .

### 3.2 Finite element model of the bridge

2D bridge finite element models cannot capture the transverse effects (e.g., failure of the spandrel walls) and the three-dimensional (3D) failure modes. To overcome these inherent limitations, 3D modelling approaches need to be deployed, although these are more computationally demanding (Zhang 2015). 3D modelling is considered in this study. The three-dimensional solid model of

MalabadiBridge prepared according to the surveys and restoration project are created as shown in Fig. 10.

The finite element model of the bridge is created using 72030 C3D8 hexagonal solid elements and 100041 nodal points in Abaqus (2010). Element size of 0.50 m is implemented for the numerical analysis. Three-dimensional finite element model of the bridge is given in Fig. 11. Due to the high nonlinear analyses time, the main part of the bridge until the fractured axis shown in Fig. 7 is considered in the finite element modelling. Due to the foundations of the bridge are supported on the rock, soil-structure interaction is not considered in the analyses, and support conditions of the foundation are chosen as fixed. Horizontal movements along the bridge length on the fractured points in Fig. 7 are prevented in the model. The surface interaction at the interface between backfill and the masonry assembly of the spandrel walls is important to capture the relative movement of the components. Cohesive nonlinear surface-based behavior allowing separation and plastic sliding is considered in the backfill-arch and the backfill-spandrel

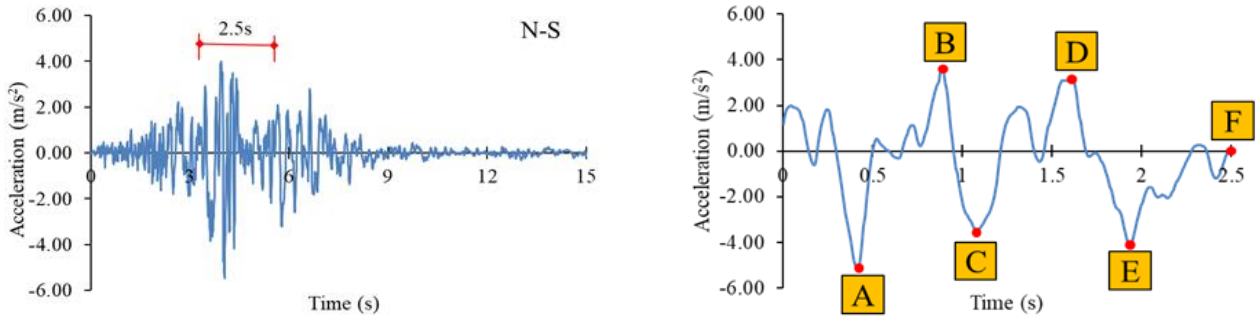


Fig. 13 North-South (N-S) components of acceleration record of May 1, 2003 Bingöl, Turkey, earthquake (Web-4 (2018))

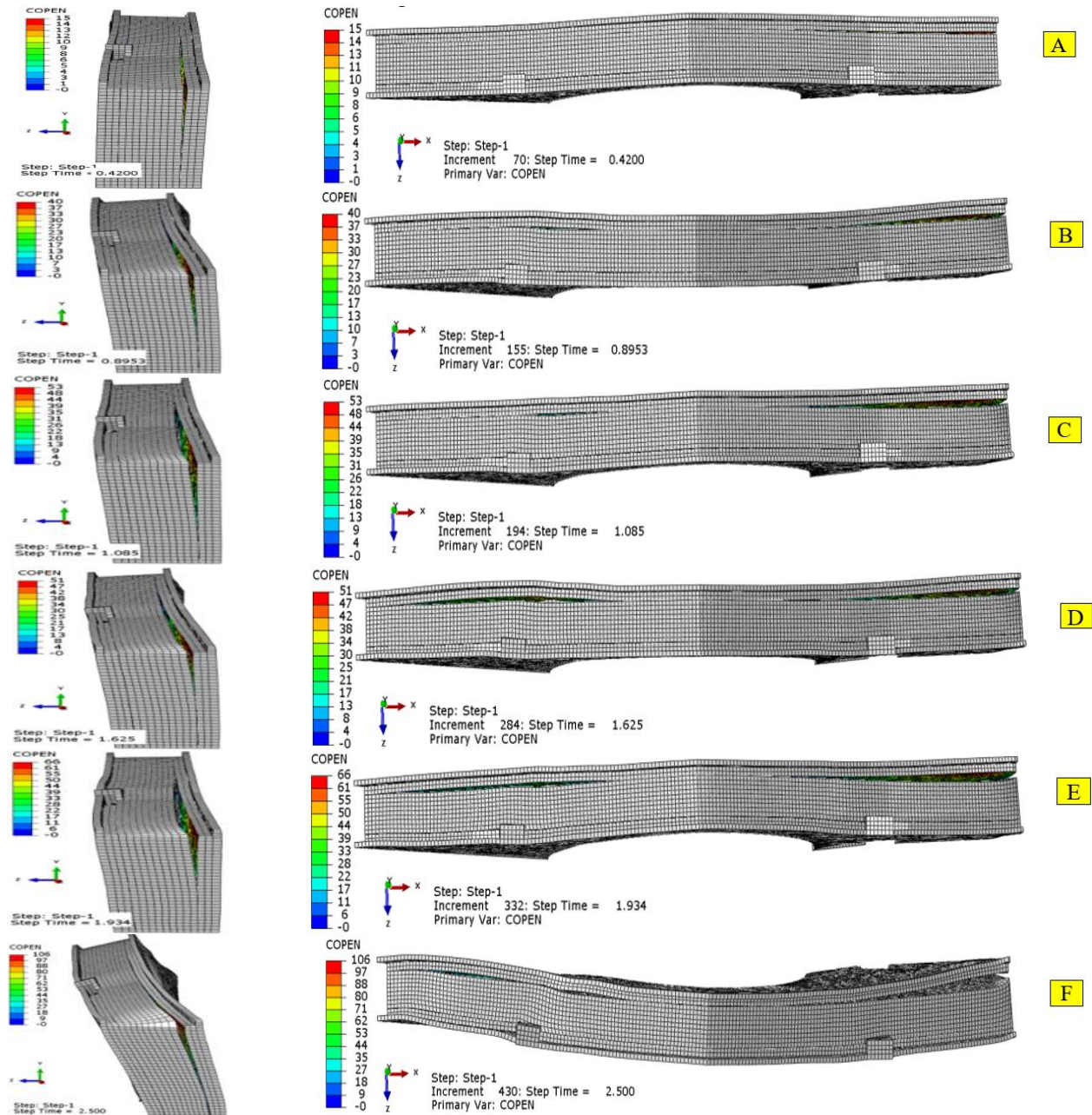


Fig. 14 Opening of spandrel walls with cohesive interface during the earthquake

wall interfaces in this study as a discontinuity. Masonry units are modelled using CDP model. The mechanical properties of the masonry units and the interfaces used in

the finite element model are given in Table 1.

### 3.3 Modal response of the bridge

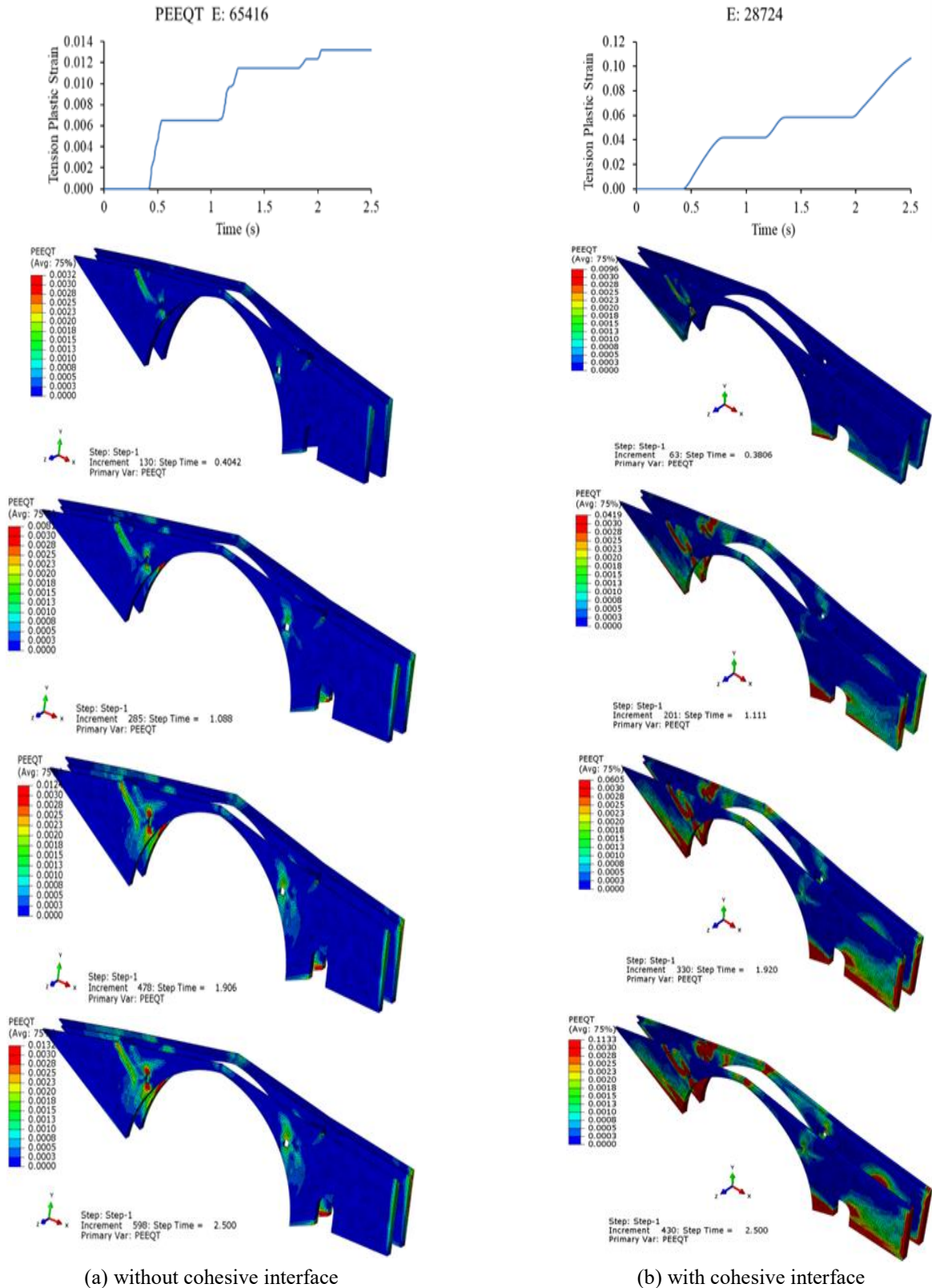


Fig. 15 Maximum principal (tension) strain contour maps of the bridge with and without cohesive interface between the fill and spandrel walls and arch

Frequencies and mode shapes of the bridge with and without cohesive interface contact are determined from the modal analyses considering the linear mechanical characteristics of the masonry units and interfaces. The first

three mode shapes of the bridge with and without cohesive interface between fill and spandrel walls and arch are compared in Fig. 12. The first, second and third frequencies vary between 2.9795-2.8041 Hz, 4.9406-4.6843 Hz and

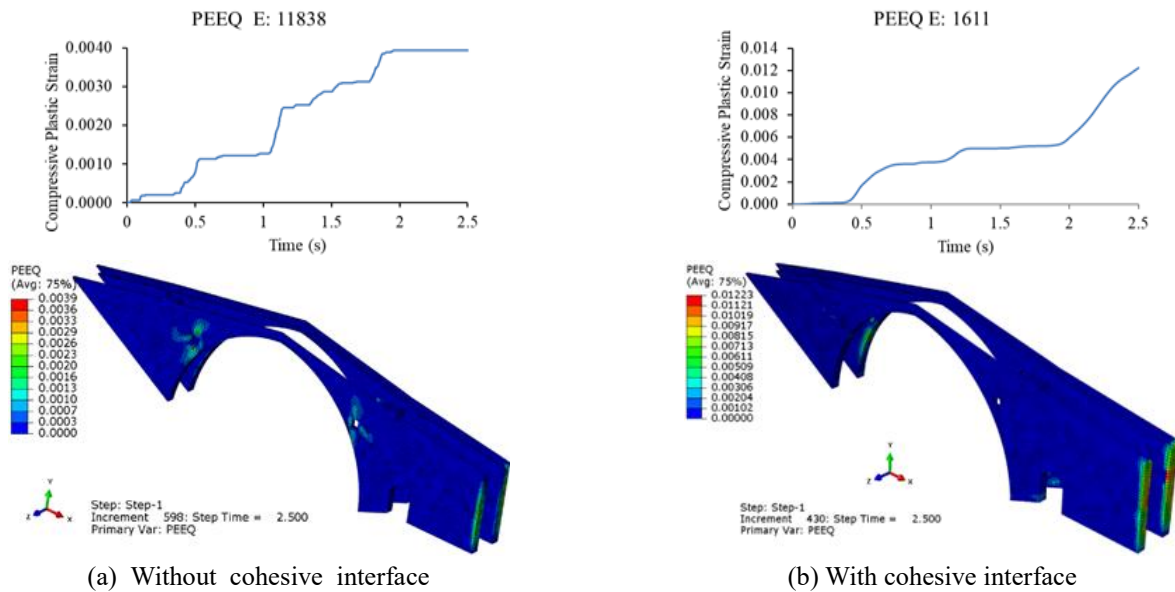


Fig.16 Minimum principal (compression) strains contour maps of the bridge with and without cohesive interface between the fill and spandrel walls and arch

6.7920-5.9178 Hz, respectively. The frequencies of the bridge decrease slightly with considering the interaction between the units. It can be seen from Fig. 12 that the first and second modes obtained from the models with and without cohesive interfaces occur in transverse direction. However, the third mode occurs in the vertical direction. Besides, it can be said that the first two modes are more effective on the out-of-plane responses of the spandrel walls.

### 3.4 Seismic response of the bridge

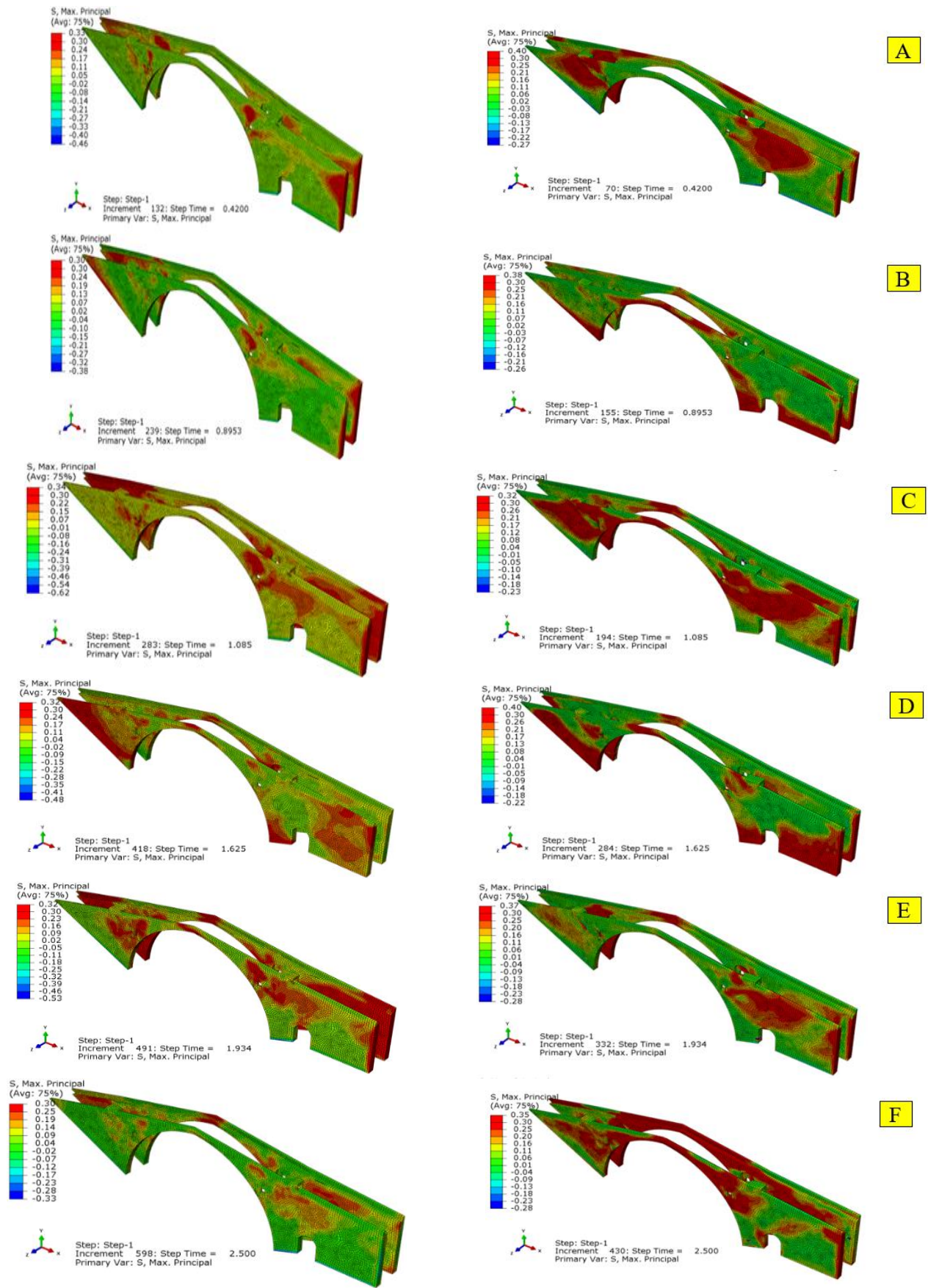
The strong ground motion record of Bingöl, Turkey, earthquake ( $M_w=6.4$ ) on May 1, 2003, which was occurred the nearest the province of Diyarbakır, is chosen for the seismic analysis of the bridge. The acceleration record of North-South (N-S) component is shown in Fig. 13. Maximum horizontal acceleration values of the acceleration record are  $5.46 \text{ m/s}^2$ . In the nonlinear seismic analyses, the N-S component of the earthquake is applied to the bridge in transverse ( $z$ ) (upstream-downstream) direction. Due to analyses time, the 2.5 s of the record given in Fig. 13 are considered in the analyses with and without cohesive interfaces between the fill and the spandrel walls and the arch.

When the cohesive interface is considered, opening between the spandrel walls and the fill in transverse direction ( $z-z$ ) for different time steps of the earthquake record is depicted in Fig. 14. A, B, C, D, E and F letters in Fig. 14 correspond to the maximum accelerations given in Fig. 13. It can be seen from Fig. 14 that openings between the spandrel walls and the fill for time step 0.42 s, 0.8953 s, 1.085 s, 1.625 s, 1.934 s and 2.5 s are determined 15 mm, 40 mm, 53 mm, 51 mm, 66 mm and 110 mm, respectively. The first opening failure starts at 0.42 second of the earthquake. The openings increase with increasing time of the earthquake record and occur almost along the interfaces

between the spandrel walls and the fill. Transverse openings are more common in areas where the spandrel walls are high.

Time histories and contour maps of maximum principal (tension) strains with and without cohesive interface between the fill and the spandrel walls are shown in Fig. 15 for different time steps. It can be seen from the time histories of principal tension strains that they considerably increase when the cohesive interface is considered in the analyses. The maximum values of the principal tension strains on the spandrel walls increase from 0.0132 to 0.1133. Besides, it can be seen from the principal (tension) strain contour maps that the strains spread wider on area of the spandrel walls and exceed the allowable strain values when the cohesive interface are considered. However, it can be seen from Fig. 16 that consideration of the cohesive interface affects less the minimum principal (compression) strains on the spandrel walls.

The maximum principal (tension) stress contour maps of the bridge with and without cohesive interfaces between the fill and the spandrel walls are given in Fig. 17 for different time steps. The maximum principal (tension) stresses increase from 0.30MPa to 0.40MPa when the cohesive interfaces are taken into account in between the spandrel wall and the fill. It is can be seen from Fig. 17 that principal tension stresses with cohesive interfaces exceed allowable tension stress value almost all over the spandrel walls when the principal tension stress contour maps with and without cohesive interfaces are compared in the end of the whole earthquake loading. However, minimum principal (compression) stresses obtained with and without cohesive interfaces between the fill and the spandrel walls do not exceed the allowable compression stress value (Fig. 18). Besides, it is stated from Fig. 18 that considering the cohesive interfaces in the analyses affects the compressive stresses slightly.



(a) Without cohesive interface

(b) With cohesive interface

Fig. 17 Maximum principal (tension) stress contour maps of the bridge with and without cohesive interface between the fill and spandrel walls and arch

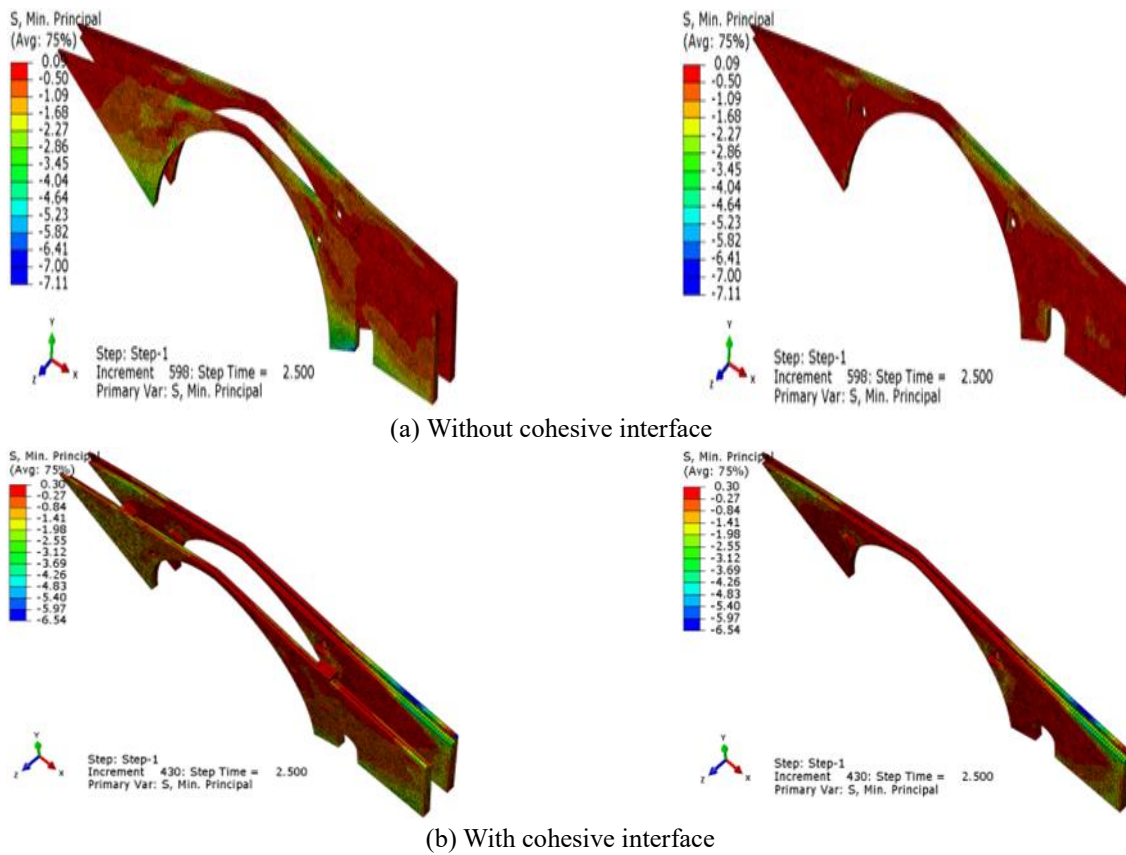


Fig. 18 Minimum principal (compression) stresses contour maps of the bridge with and without cohesive interface between the fill and spandrel walls and arch

#### 4. Conclusions

Out-of-plane seismic failure responses of the spandrel walls of a long-span and high masonry stone arch bridge have been determined in this study. CDP material model and the cohesive interface allowing separation and plastic sliding between the spandrel walls and the backfill and the arch were considered in the 3D nonlinear time history analyses. Based on the nonlinear finite element analyses of spandrel walls of masonry stone arch bridges, the following conclusions can be drawn from the present study:

- The most vulnerable structural element under transverse seismic loads is the spandrel walls. Therefore, a realistic representation of the backfill behavior and its interaction with the arch barrel and the spandrel walls is critical for an accurate response prediction of masonry arch bridges.
- Interface stiffness between spandrel wall and backfill is an important parameter that affects the behavior of the spandrel walls.
- Frequencies of the masonry stone arch bridge slightly decrease when the interface interaction between the spandrel wall and the backfill is considered in the finite element model. The first and second modes occur in transverse direction; however the third mode occurs in vertical direction for both with and without cohesive interfaces. It can be said that the first two modes are more effective on the transverse responses of spandrel walls.

- When the cohesive interface is considered, the openings increase with increasing time of the earthquake record and occur almost along the interfaces between the spandrel walls and the backfill.
- The values of the principal tension strains and stresses on the spandrel walls considerably increase when the cohesive interface is considered in the finite element models. Besides, the principal tension strain and stresses contour maps spread over a wider area on the spandrel walls and exceed the allowable values. However, consideration of the cohesive interface less affects the principal compression strains and stresses on the spandrel walls.

It is seen from the results obtained that the out-of-plane responses of the masonry spandrel walls with the interface interactions are very sensitive to the transverse earthquake forces. Therefore, it is recommended that the interface interactions between the spandrel walls and the infill and the arch should be considered in the out-of-plane seismic failure assessments of the masonry arch bridges with long-span and high spandrel walls.

#### Acknowledgments

The authors would like to express sincere thanks to General and Regional Directorates of Highways in Ankara and Diyarbakır, Turkey, for their contributions.

## Conflict of Interest

The authors declare that they have no conflict of interest.

## References

- Abdulla, K., Cunningham, L. and Gillie, M. (2017), "Simulating masonry wall behaviour using a simplified micro-model approach", *Eng. Struct.*, **151**(15), 349-365. <https://doi.org/10.1016/j.engstruct.2017.08.021>.
- Ali, S.S. and Page, A.W. (1988), "Finite element model for masonry subjected to concentrated loads", *J. Struct. Eng.*, **114**(8), 1761-1784. [https://doi.org/10.1061/\(ASCE\)0733-9445\(1988\)114:8\(1761\)](https://doi.org/10.1061/(ASCE)0733-9445(1988)114:8(1761)).
- Altunisik, A.C., Bayraktar, A. and Genc, A.F. (2015), "Determination of the restoration effect on the structural behavior of masonry arch bridges", *Smart Struct. Syst.*, **16**(1), 101-139. <http://dx.doi.org/10.12989/sss.2015.16.1.101>.
- Altunisik, A.C., Bayraktar, A., Sevim, B. and Birinci F. (2011), "Vibration-based operational modal analysis of the Mikron historic arch bridge after restoration", *Civil Eng. Environ. Syst.*, **28**(3), 247-259. <https://doi.org/10.1080/10286608.2011.588328>.
- Aras, F. and Altay, G. (2015), "Investigation of mechanical properties of masonry in historic buildings", *Građevinar*, **67**(5), <https://doi.org/10.14256/JCE.1145.2014>.
- Ataci, S., Miri, A. and Jahangiri, M. (2017), "Assessment of load carrying capacity enhancement of an open spandrel masonry arch bridge by dynamic load testing", *Int. J. Arch. Herit.*, **11**(8), 1086-1100. <https://doi.org/10.1080/15583058.2017.1317882>.
- Aydin, A.C. and Özkaya, S.G. (2018), "The finite element analysis of collapse loads of single-spanned historic masonry arch bridges (Ordu, Sarpdere Bridge)", *Eng. Fail. Anal.*, **84**, 131-138. <https://doi.org/10.1016/j.engfailanal.2017.11.002>.
- Bayraktar, A., Altunisik, A.C., Birinci, F., Sevim, B. and Türker, T. (2010), "Finite-element analysis and vibration testing of a two-span masonry arch bridge", *J. Perform. Constr. Facil.*, **24**(1), 46-52. [https://doi.org/10.1061/\(ASCE\)CF.1943-5509.0000060](https://doi.org/10.1061/(ASCE)CF.1943-5509.0000060).
- Bayraktar, A., Birinci, F., Altunisik, A.C., Türker, T. and Sevim, B. (2009), "Finite element model updating of Senyuva historical arch bridge using ambient vibration tests", *Balt. J. Road Bridge Eng.*, **4**(4), 177-185. <https://doi.org/10.3846/1822-427X.2009.4.177-185>.
- Bayraktar, A., Türker, T. and Altunisik, A.C. (2015), "Experimental frequencies and damping ratios for historical masonry arch bridges", *Constr. Build. Mater.*, **75**(30), 234-241. <https://doi.org/10.1016/j.conbuildmat.2014.10.044>.
- Bolhassani, M., Hamid, A.A., Lau, A.C.W. and Moon, F. (2015), "Simplified micro modeling of partially grouted masonry assemblages", *Constr. Build. Mater.*, **83**(15), 159-173. <https://doi.org/10.1016/j.conbuildmat.2015.03.021>.
- Boothby, T.E. (2001), "Analysis of masonry arches and vaults", *Prog. Struct. Eng. Mater.*, **3**(3), 246-256. <https://doi.org/10.1002/pse.84>.
- Camanho, P.O. and Dávila, C.G. (2002), "Mixed-mode decohesion finite elements for the simulation of delamination in composite materials", Report No. 20020053651, NASA Langley Research Center, Varginia, U.S.A.
- Casolo, S. (1999), "Rigid element model for non-linear analysis of masonry façades subjected to out-of-plane loading", *Commun. Numer. Meth. Eng.*, **15**(7), 457-468. [https://doi.org/10.1002/\(SICI\)10990887\(199907\)15:7<457::AID-CNEM259>3.0.CO;2-W](https://doi.org/10.1002/(SICI)10990887(199907)15:7<457::AID-CNEM259>3.0.CO;2-W).
- Cavalagli, N., Gusella, V. and Severini L. (2016), "Lateral loads carrying capacity and minimum thickness of circular and pointed masonry arches", *Int. J. Mech. Sci.*, **115-116**, 645-656. <https://doi.org/10.1016/j.ijmecsci.2016.07.015>.
- Cavicchi, A. and Gambarotta, L. (2005), "Collapse analysis of masonry bridges taking into account arch-fill interaction", *Eng. Struct.*, **27**(4), 605-615. <https://doi.org/10.1016/j.engstruct.2004.12.002>.
- Cavicchi, A. and Gambarotta, L. (2007), "Lower bound limit analysis of masonry bridges including arch-fill interaction", *Eng. Struct.*, **29**(11), 3002-3014. <https://doi.org/10.1016/j.engstruct.2007.01.028>.
- Chajes, M. (2002), *Load Rating of Arch Bridges*, Delaware Center for Transportation, University of Delaware, Delaware, U.S.A.
- Costa, C., Arêde, A., Morais, M. and Anibal, A. (2015), "Detailed FE and DE modelling of stone masonry arch bridges for the assessment of load-carrying capacity", *Procedia Eng.*, **114**, 854-861. <https://doi.org/10.1016/j.proeng.2015.08.039>.
- Costa, C., Ribeiro, D., Jorge, P., Silva, R., Arêde, A. and Caçada, R. (2016), "Calibration of the numerical model of a stone masonry railway bridge based on experimentally identified modal parameters", *Eng. Struct.*, **123**(15), 354-371.
- Dassault Systèmes Simulia Corp. (2010), Abaqus v13, Providence, Rhode Island, U.S.A.
- Disaster and Emergency Management Authority Presidential Earthquake Department (2019), AFAD Earthquakes, <http://www.deprem.gov.tr/en/Category/earthquake-zoning-map-96531>.
- Disaster and Emergency Management Authority Presidential of Earthquake Department (2019), AFAD Earthquakes, Web-4, <http://www.deprem.gov.tr/en/home>.
- Doherty, K. (2000), "An investigation of the weak links in the seismic load path of unreinforced masonry building", Ph.D. Thesis, University of Adelaide, Adelaide, Australia.
- Erdogmus, E. and Boothby, T. (2004), "Strength of Spandrel Walls in Masonry Arch Bridges", *Tran. Res. Rec. J. Transp. Res. Board*, **1892**(1), 47-55. <https://doi.org/10.3141/1892-06>.
- Eurocode 6. (1996), Design of Masonry Structures, European Union, Brussel, Belgium.
- Fanning, P., Boothby, T.E. and Roberts, B.J. (2001), "Longitudinal and transverse effects in masonry arch assessment", *Constr. Build. Mater.*, **15**(1), 51-60. [https://doi.org/10.1016/S0950-0618\(00\)00069-6](https://doi.org/10.1016/S0950-0618(00)00069-6).
- Fanning, P.J. and Boothby, T.E. (2001), "Three-dimensional modelling and full-scale testing of stone arch bridges", *Comput. Struct.*, **79**(29-30), 2645-2662. [https://doi.org/10.1016/S0045-7949\(01\)00109-2](https://doi.org/10.1016/S0045-7949(01)00109-2).
- Gago, A.S., Alfaiate, J. and Lamas, A. (2011), "The effect of the infill in arched structures: Analytical and numerical modelling", *Eng. Struct.*, **33**(5), 1450-1458. <https://doi.org/10.1016/j.engstruct.2010.12.037>.
- Gullu, H. and Jaf, H.S. (2016), "Full 3D nonlinear time history analysis of dynamic soil-structure interaction for a historical masonry arch bridge", *Environ. Earth Sci.*, **75**, 1421. <https://doi.org/10.1007/s12665-016-6230-0>.
- Karaton, M., Aksoy, H.S., Sayın, E. and Calayır, Y. (2017), "Nonlinear seismic performance of a 12th century historical masonry bridge under different earthquake levels", *Eng. Fail. Anal.*, **79**, 408-421. <https://doi.org/10.1016/j.engfailanal.2017.05.017>.
- Kaushik, H.B., Rai, D.C. and Jain, S.K. (2007), "Stress-strain characteristics of clay brick masonry under uniaxial compression", *J. Mater. Civil Eng.*, **19**(9), 728-739. [https://doi.org/10.1061/\(ASCE\)0899-1561\(2007\)19:9\(728\)](https://doi.org/10.1061/(ASCE)0899-1561(2007)19:9(728)).
- Kowalewski, L. and Gajewski, M. (2015), "Determination of failure modes in brick walls using cohesive elements", *Procedia Eng.*, **111**, 454-461. <https://doi.org/10.1016/j.proeng.2015.07.116>.
- Lancioni, G., Gentilucci, D., Quagliarini, E. and Lenci, S. (2016), "Seismic vulnerability of ancient stone arches by using a

- numerical model based on the non-smooth contact dynamics method”, *Eng. Struct.*, **119**(15), 110-121. <https://doi.org/10.1016/j.engstruct.2016.04.001>.
- Loo, Y.C. and Yang, Y. (1991), “Cracking and failure analysis of masonry arch bridges”, *J. Struct. Eng.*, **117**(6), 1641-1659. [https://doi.org/10.1061/\(ASCE\)0733-9445\(1991\)117:6\(1641\)](https://doi.org/10.1061/(ASCE)0733-9445(1991)117:6(1641)).
- Lourenço, P.B. (1996), “Computational strategies for masonry structures”, TU Delft, Delft University of Technology, The Delft, Netherlands.
- Lourenço, P.B. and Rots, J.G. (1997), “Multi surface interface model for analysis of masonry structures”, *J. Eng. Mech.*, **123**(7), 660-668. [https://doi.org/10.1061/\(ASCE\)0733-9399\(1997\)123:7\(660\)](https://doi.org/10.1061/(ASCE)0733-9399(1997)123:7(660)).
- Macorini, L. and Izzuddin, B.A. (2011), “A non-linear interface element for 3D mesoscale analysis of brick-masonry structures”, *Int. J. Numer. Meth. Eng.*, **85**(12), 1584-1608. <https://doi.org/10.1002/nme.3046>.
- Martinelli, P., Galli, A., Barazzetti, L., Colombo, M., Felicetti, R., Previtali, M., Roncoroni, F., Scola, M. and di Prisco, M. (2017), “Bearing capacity assessment of a 14th century arch bridge in Lecco (Italy)”, *Int. J. Archit. Herit.*, **12**(2), 237-256. <https://doi.org/10.1080/15583058.2017.1399482>.
- Michiels, T. and Adriaenssens, S. (2018), “Form-finding algorithm for masonry arches subjected to in-plane earthquake loading”, *Comput. Struct.*, **195**(15), 85-98. <https://doi.org/10.1016/j.compstruc.2017.10.001>.
- Milani, G. and Lourenço, P.L. (2012), “3D non-linear behavior of masonry arch bridges”, *Comput. Struct.*, **110-111**, 133-150. <https://doi.org/10.1016/j.compstruc.2012.07.008>.
- Milani, G. and Tralli, A. (2011), “Simple SQP approach for out-of-plane loaded homogenized brickwork panels, accounting for softening”, *Comput. Struct.*, **89**(1-2), 201-215. <https://doi.org/10.1016/j.compstruc.2010.09.005>.
- Moreira, V.N., Matos, J.C. and Oliveira, D.V. (2017), “Probabilistic-based assessment of a masonry arch bridge considering inferential procedures”, *Eng. Struct.*, **134**(1), 61-73. <https://doi.org/10.1016/j.engstruct.2016.11.067>.
- Naderi, M. and Zekavati, M. (2018), “Assessment of seismic behavior stone bridge using a finite element method and discrete element method”, *Earthq. Struct.*, **14**(4), 297-303. <https://doi.org/10.12989/eas.2018.14.4.297>.
- Orduna, A. (2005), “Seismic assessment of ancient masonry structures by rigid blocks limit analysis”, Ph.D. Thesis, University of Minho, Braga, Portugal.
- Öztürk, Ş., Bayraktar, A., Hökelekli, E. and Ashour, A. (2019), “Nonlinear structural performance of a historical brick masonry inverted dome”, *Int. J. Arch. Herit.*, 1-19. <https://doi.org/10.1080/15583058.2019.1592265>.
- Page, J. (1993), “Repair and strengthening of arch bridges”, *Proceedings of the IABSE Symposium: Structural Preservation of the Architectural Heritage*, Rome, Italy, September.
- Porto, F., Tecchio, G., Zampieri, P., Modena, C. and Prot, A. (2016), “Simplified seismic assessment of railway masonry arch bridges by limit analysis”, *Struct. Infrastr. Eng.*, **12**(5), 567-591. <https://doi.org/10.1080/15732479.2015.1031141>.
- Restoration Project (2014), “Malabadi bridge report”, Diyarbakır, Turkey.
- Rota, M. (2004), “Seismic vulnerability of masonry arch bridge walls”, M.Sc. Thesis, University of Pavia, Pavia, Italy.
- Rota, M., Pecker, A., Bolognini, D. and Pinho, R. (2005), “A methodology for seismic vulnerability of masonry arch bridge walls”, *J. Earthq. Eng.*, **9**(2), 331-353. <https://doi.org/10.1142/S1363246905002432>.
- Sacco, E. and Toti, J. (2010), “Interface elements for the analysis of masonry structures”, *Int. J. Comput. Meth. Eng. Sci. Mech.*, **11**(6), 354-373.
- Salih, S.A. (2018), “Rate-dependent cohesive-zone models for fracture and fatigue”, Ph.D. Thesis, University of Manchester, Manchester, England, U.K.
- Sarhosis, V., De Santis, S. and de Felice, G. (2016), “A review of experimental investigations and assessment methods for masonry arch”, *Struct. Infrastr. Eng.*, **12**(11), 1439-1464. <http://dx.doi.org/10.1080/15732479.2015.1136655>.
- Sert, H., Yılmaz, S., Partal, E.M., Demirci, H., Avşın, A., Nas, M., Turan, S. (2015) “Tarihi Malabadi (Batman Su) Köprüsü’nde Yürütülen Restorasyon-Konservasyon Çalışmaları, 5. Tarihi Eserlerin Güçlendirilmesi ve Geleceğe Güvenle Devredilmesi Sempozyumu, 1-2 Ekim 2015”, 144-153, Erzurum, Turkey. (in Turkish)
- Severini, L., Cavalagli, N., DeJong, M. and Gusella, V. (2018), “Dynamic response of masonry arch with geometrical irregularities subjected to a pulse-type ground motion”, *Nonlin. Dyn.*, **91**, 609-624. <https://doi.org/10.1007/s11071-017-3897-z>.
- Sevim, B., Atamturktur, S., Altunişik, A.C. and Bayraktar, A. (2016), “Ambient vibration testing and seismic behavior of historical arch bridges under near and far fault ground motions”, *Bull. Earthq. Eng.*, **14**, 241-259. <https://doi.org/10.1007/s10518-015-9810-6>.
- Sevim, B., Bayraktar, A., Altunişik, A.C., Atamtürktür, S. and Birinci, F. (2011a), “Finite element model calibration effects on the earthquake response of masonry arch bridges”, *Fin. Elem. Anal. Des.*, **47**(7), 621-634. <https://doi.org/10.1016/j.finel.2010.12.011>.
- Sevim, B., Bayraktar, A., Altunişik, A.C., Atamtürktür, S. and Birinci, F. (2011b), “Assessment of nonlinear seismic performance of a restored historical arch bridge using ambient vibrations”, *Nonlin. Dyn.*, **63**, 755-770. <https://doi.org/10.1007/s11071-010-9835-y>.
- Shi, Y.N. (2016), “Dynamic behaviour of Masonry structures”, Ph.D. Dissertation, University of Bath, Bath, U.K.
- Stavroulaki, M.E., Riveiro, B., Drosopoulos, G.A., Solla, M., Koutsianitis, P. and Stavroulakis, G.E. (2016), “Modelling and strength evaluation of masonry bridges using terrestrial photogrammetry and finite elements”, *Adv. Eng. Softw.*, **101**, 136-148. <https://doi.org/10.1016/j.advengsoft.2015.12.007>.
- Thompson, D.R. (1995), “Assessment of spandrel walls. Arch bridge”, *Proceedings of the 1st International Conference on Arch Bridges*, Bolton, U.K., September.
- UIC Code 778-3R (1994), “Recommendations for the inspection, assessment and maintenance of masonry arch bridges”, International Union of Railways, Paris, France.
- UNESCO (2018), UNESCO global strategy tentative lists, UNESCO, Paris, France. <https://whc.unesco.org/en/tentativelists/6113>.
- Wang, J. (2014), “Numerical modelling of masonry arch bridges: Investigation of spandrel wall failure”, Ph.D. Thesis, University of Bath, Bath, U.K.
- Zampieri, P., Faleschini, F., Zanini, M.A., Simoncello, N. (2018), “Collapse mechanisms of masonry arches with settled springing”, *Eng. Struct.*, **156**(1), 363-374. <https://doi.org/10.1016/j.engstruct.2017.11.048>.
- Zampieri, P., Tecchio, G., da Porto, F. and Modena, C. (2015), “Limit analysis of transverse seismic capacity of multi-span masonry arch bridges”, *Bull. Earthq. Eng.*, **13**, 1557-1579. <https://doi.org/10.1007/s10518-014-9664-3>.
- Zhang, Y. (2015), “Advanced nonlinear analysis of masonry arch bridges”, Ph.D. Thesis, Imperial College London, London, U.K.
- Zhang, Y., Macorini, L. and Izzuddin, B.A. (2018), “Numerical investigation of arches in brick-masonry bridges”, *Struct. Infrastr. Eng.*, **14**(1), 14-32. <https://doi.org/10.1080/15732479.2017.1324883>.